

# NUMERICAL MODELING OF AN FGM BEAM USING THE FINITE ELEMENT METHOD

H. ZIOU<sup>(1)</sup>, H. GUENFOUD<sup>(2)</sup>, M. HIMEUR<sup>(3)</sup>, M. GUENFOUD<sup>(4)</sup>

<sup>(1)</sup>Department of Civil Engineering, University of Biskra, B.P. 145, R.P. 07000, Biskra, Algeria  
hassina.geniecivil@gmail.com

<sup>(2,3,4)</sup>LGCH Laboratory, University of 08 may 1945, Guelma, Algeria  
hamzaguenfoud@gmail.com  
bet\_himeur@yahoo.fr  
Guenfoud.mohamed@univ-guelma.dz

## ABSTRACT

In this paper, a finite element procedure for static analysis of functionally graded material (FGM) beam is presented. The material properties of the beam are assumed to vary continuously along the beam thickness by a power-law distribution. The assumed field displacements equations of the beam are represented by Euler-Bernoulli and first order shear deformation theories. A simply supported beam subjected to uniform load for different length-to-thickness ratio has been chosen. The influences of span-to-depth and the volume fraction index on the mid plane deflections, and stresses distribution along the thickness of the beam are examined. The obtained results are compared with the existing solutions to verify the validity of the developed theories.

**KEYWORDS:** Functionally Graded Material; Power-law; Finite Element Method; Euler Bernoulli's beam; Timoshenko's beam.

## 1 INTRODUCTION

Functionally graded materials (FGM's) are a new kind of composite materials which have a gradual and continuous variation of the volume fraction of each component (usually metal and ceramic) through the thickness direction, leading to changes of global thermo mechanical properties of the structural element they represent. They were designed to overcome the problems caused by severe thermal environments.

A new beam element based on the first order shear deformation theory was developed to study the thermo elastic behavior of FGM beam structures by Chakraborty and Gopalakrishnan [1], Chakraborty et al. [2] In those papers; both exponential and power variations of material property distribution were employed. Kapuria et al. [3] presented a finite element model for static and free vibration responses of layered FG beams using an efficient third order zigzag theory for estimating the effective modulus of elasticity, and its experimental validation for two different FGM systems under various boundary conditions. Kadoli et al. [4] proposed a finite element based on a third-order approximation of the axial displacement and constant transverse displacement for the static analysis of beams made of metal-ceramic FGMs. Components' volume fraction was supposed to vary according to a power-law function. A discrete layer approach was adopted to account for material gradation. As far as elasticity

solutions are concerned. Shi et al. [5] presented the quasi-conforming finite element for the deflection analysis of composite beams using higher order theory. Kutiš et al. [6] presented a finite element procedure for modeling a FGM beam with spatial variation of material properties. Also using the finite element method, Pindera and Dunn [7] evaluated the higher order theory by performing a detailed finite element analysis of the FGM. They found that the HOTFGM results agreed well with the FE results. The large deflections of tapered functionally graded beams subjected to end forces are studied by Nguyen and Gan [8] by using the finite element method. The material properties of the beams are assumed to vary through the thickness direction according to a power law distribution. The finite element formulation of the FG beam element derived in the present paper has been applied in a finite element program. Using this program, some sample problems are solved to show the performance of the present finite element FG beam formulation. The material properties of the beam are assumed to vary continuously along the beam thickness by a power-law distribution. The assumed field displacements equations of the beam are represented by Euler-Bernoulli and first order shear deformation theories. A simply supported beam subjected to uniform load for different length-to-thickness ratio has been chosen. The influences of span-to-depth and the volume fraction index on the mid plane deflections, and stresses distribution along the thickness of the beam are examined. The obtained results

are compared with the existing solutions to verify the validity of the developed theories.

## 2 MATERIAL PROPERTIES OF FGM BEAM AND FINITE ELEMENT FORMULATION

### 2.1 Effective material properties of metal ceramic functionally graded beams

(Fig.1) shows a FGM beam composed of ceramic and metal of length L, width b and thickness h. Material properties vary continuously in the z direction. Topmost surface consists of only ceramic and bottom surface has only metal. In between volume fraction of ceramic  $V_c$  and metal  $V_m$  are obtained by power law distribution in conjunction with simple law of constituent mixture as follows:

$$V_m = \left(\frac{z}{h} + \frac{1}{2}\right)^p \quad (1-a)$$

$$V_c = 1 - V_m \quad (1-b)$$

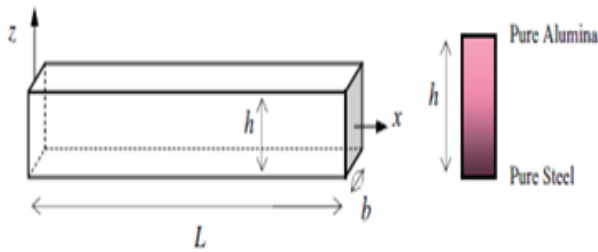


Figure 01: Geometry of FGM beam and the possible variation of ceramic and metal through thickness

Where,

$z$  = distance from mid-surface and  $p$  = power law index, the non-negative variable parameter which dictates the material variation profile through the thickness of the beam a positive real number. For  $p = 0$  volume fraction of ceramic becomes one and homogeneous beam consisting only ceramic is obtained, when value of  $p$  is increased, content of metal in FGM increases.

The effective material properties  $MP_{eff}$  corresponding to the model of Voigt (Shen, 2009) are evaluated using the relation:

$$MP_{eff} = MP_m V_m(z) + MP_c V_c(z) \quad (2)$$

Where,  $MP_m$  and  $MP_c$  stands for material properties of metals and ceramics respectively. Thus the modulus of elasticity  $E_{eff}$ , Poisson's ratio  $\nu_{eff}$ , and shear modulus  $G_{eff}$ , of FGMs can be given a by a simple power law distribution

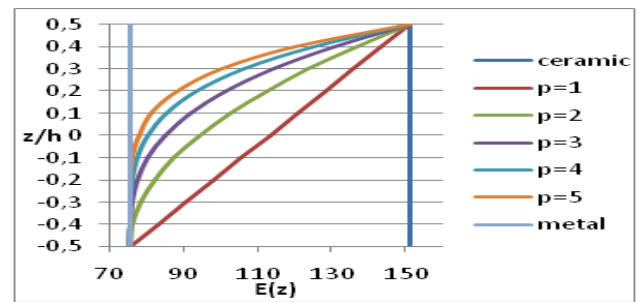
(Simsek, 2009):

$$E_{eff} = (E_c - E_m) \left(\frac{z}{h} + \frac{1}{2}\right)^p + E_m \quad (3-a)$$

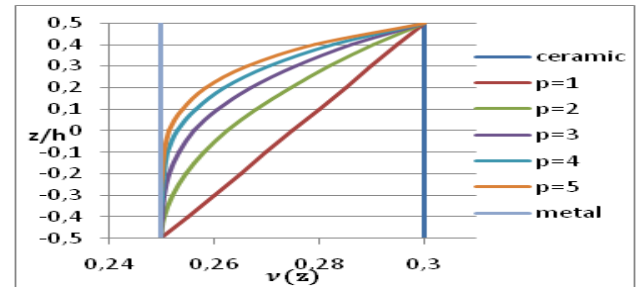
$$\nu_{eff} = (\nu_c - \nu_m) \left(\frac{z}{h} + \frac{1}{2}\right)^p + \nu_m \quad (3-b)$$

$$G_{eff} = (G_c - G_m) \left(\frac{z}{h} + \frac{1}{2}\right)^p + G_m \quad (3-c)$$

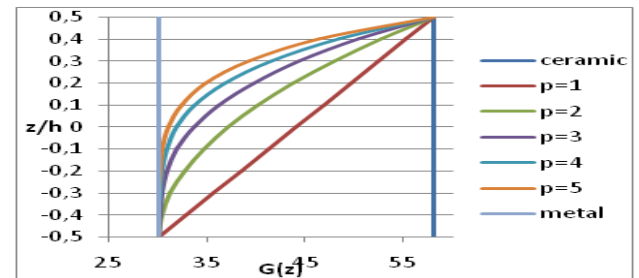
Using the above relation it is possible to obtain an insight into the variation of the material properties across the thickness of the beam for different power law indexes. (Fig. 2a, 2b, 2c) illustrate the variation of Young's modulus and Poisson's ratio and shear modulus of an FGM beam.



a) Young's Modulus  $E(z)$



b) Poisson's ratio  $\nu(z)$



c) Shear Modulus  $G(z)$

Figure 02: Variation of Poisson's ratio, Young's modulus and Shear Modulus of an FGM beam along the thickness for various power law indexes

## 2.2 Finite element formulation

### 2.2.1 Euler-Bernoulli beam (CBT)

Based on the Euler–Bernoulli beam theory, the axial displacement  $u$  and the transverse displacement of any point of the beam,  $w$ , are given by:

$$u(x, z) = u_0(x) - z \frac{\partial w_0(x)}{\partial x} \quad (4-a)$$

$$w(x, z) = w_0(x) \quad (4-b)$$

Eqs. (4) Can be rewritten as

$$\{u(M)\} = \begin{Bmatrix} u \\ w \end{Bmatrix} = \begin{bmatrix} 1 & 0 & -z \\ 0 & 1 & 0 \end{bmatrix} \begin{Bmatrix} u_0 \\ w_0 \\ \frac{\partial w_0}{\partial x} \end{Bmatrix} \quad (5)$$

Where  $u_0$  and  $w_0$  are the axial and the transverse displacement of any point on the mid-plane.

By assuming the small deformations, the displacement–strain relation can be represented by

$$\varepsilon_{xx} = \frac{\partial u_0}{\partial x} - z \frac{\partial^2 w_0}{\partial x^2} = \varepsilon_{xx}^0 - z \kappa_{xx}^0 \quad (6-a)$$

$$\varepsilon_{xx} = \begin{bmatrix} 1 & -z \end{bmatrix} \begin{Bmatrix} \frac{\partial u_0}{\partial x} \\ \frac{\partial^2 w_0}{\partial x^2} \end{Bmatrix} \quad (6-b)$$

Where  $\varepsilon_{xx}$  is the normal strain in the x direction.

Considering the material of FGM beam obeys Hooke's law, the strain–stress constitutive equation can be written as following

$$\sigma_{xx}(z) = E(z) \varepsilon_{0,xx} + z E(z) \kappa_{xx} \quad (7-a)$$

$$\sigma_{xx} = E(z) \varepsilon_{xx} = E(z) \begin{bmatrix} 1 & -z \end{bmatrix} \begin{Bmatrix} \frac{\partial u_0}{\partial x} \\ \frac{\partial^2 w_0}{\partial x^2} \end{Bmatrix} \quad (7-b)$$

The constitutive equation expressed as a function FGMs membrane forces  $N$  and bending moments  $M$  for a FGM beam, is given by

$$(N, M) = \int_{-h/2}^{+h/2} \sigma_{xx}(1, z) dz \quad (8)$$

### 2.2.2 Timoshenko beam theory (TBT)

Let us consider a straight beam of length  $L$  and axis  $x$  linking the gravity center  $G$  of all cross-sections with  $xz$  being a principal plane of inertia. The variation of material properties is along the beam thickness and assumed to follow the power-law. Hence, in general the beam axis does

not coincide with the neutral axis. Timoshenko hypothesis for the rotation of the normal to hold will be assumed. The axial and vertical displacements of a point A of the beam section are expressed as

$$u(x, z) = u_0(x) - z\phi(x) \quad (9-a)$$

$$w(x, z) = w_0(x) \quad (9-b)$$

Where  $(-)_0$  denotes the displacements of the beams axis

The axial and transverse shear strains are deduced from eqs. (9) as

$$\varepsilon_{xx} = \frac{\partial u_0}{\partial x} - z \frac{\partial \phi}{\partial x} = \varepsilon_{xx}^0 - z \kappa_{xx}^0 \quad (10-a)$$

$$\gamma_{xz} = \frac{\partial w_0}{\partial x} - \phi \quad (10-b)$$

Equation (10) can be written in matrix form as

$$\varepsilon = \begin{Bmatrix} \varepsilon_x \\ \gamma_{xz} \end{Bmatrix} = \begin{bmatrix} 1 & -z & 0 \\ 0 & 0 & 1 \end{bmatrix} \begin{bmatrix} \frac{\partial u_0}{\partial x} & \frac{\partial \phi}{\partial x} & \frac{\partial w_0}{\partial x} - \phi \end{bmatrix}^T = S \hat{\varepsilon} \quad (11-a)$$

With,

$$S = \begin{bmatrix} 1 & -z & 0 \\ 0 & 0 & 1 \end{bmatrix}, \hat{\varepsilon} = \begin{bmatrix} \frac{\partial u_0}{\partial x} & \frac{\partial \phi}{\partial x} & \frac{\partial w_0}{\partial x} - \phi \end{bmatrix}^T \quad (11-b)$$

where  $\varepsilon$  is the strain vector,  $\hat{\varepsilon}$  is the generalized strain vector containing the elongation of the beam axis  $\frac{\partial u_0}{\partial x}$ , the

curvature  $\frac{\partial \phi}{\partial x}$  and the transverse shear strain  $\frac{\partial w_0}{\partial x} - \phi$  and

$S$  is a strain-displacement transformation matrix depending on the thickness coordinate  $z$ .

From the equilibrium equation along the x direction

$$\frac{\partial \sigma_{xx}}{\partial x} + \frac{\partial \tau_{xz}}{\partial z} = 0 \rightarrow \tau_{xz}(x, z') = - \int_{\pm(h/2)-a}^{z'} \frac{\partial \sigma_{xx}}{\partial x} dz \quad (12)$$

### 2.2.3 The position of the neutral surface

Clearly, due to variation of the effective Young's modulus, the neutral axis is no longer at the midplane, but it shifts from the midplane unless for an isotropic beam with symmetrical Young's modulus. The position of the neutral axis can be determined by solving the following equation:

$$\frac{b}{\rho} \left( \int_{-h/2}^{+h/2} E(z) z dz - a \int_{-h/2}^{+h/2} E(z) dz \right) = 0 \quad (13)$$

Where,

$a$ : is the distance of the neutral surface from the midplane of beam and  $\rho$  is the curvature radius of the neutral surface.

The position of the neutral surface can be determined from below equation:

$$a = \frac{\int_{-h/2}^{+h/2} E(z)zdz}{\int_{-h/2}^{+h/2} E(z)dz} \quad (14)$$

properties of aluminum are:

$$E_m = 70GPa, \nu_m = 0.3$$

And those of alumina are  $E_m = 380GPa, \nu_m = 0.3$

The non-dimensional quantities used here are

$$\bar{w} = 100 \frac{E_m h^3}{qL^4} w\left(\frac{L}{2}, \frac{h}{2}\right), \bar{\sigma}_x = \frac{h}{qL} \sigma_x\left(\frac{L}{2}, \frac{h}{2}\right), \bar{\tau}_{xz} = \frac{h}{qL} \tau_{xz}(0,0)$$

### 3 NUMERICAL RESULTS AND DISCUSSIONS

#### 3.1 Static Analysis

In this section, various examples are presented and discussed to verify the accuracy of present theories in predicting the bending of simply supported FG beams (Fig.1). An Al/Al<sub>2</sub>O<sub>3</sub> beam composed of aluminum (metal) and alumina (ceramic) is considered. The material

Table 1 contains the nondimensional deflections and stresses of FGM beams under uniform load for different values of power law index and different span-to-depth ratio.

Table 01: Nondimensional deflections and stress of FGM beams under uniform load

p	Method	L/h=5			L/h=20		
		$\bar{w}$	$\bar{\sigma}_x$	$\bar{\tau}_{xz}$	$\bar{w}$	$\bar{\sigma}_x$	$\bar{\tau}_{xz}$
0	Li et al. [9]	31,65	38,02	7,50	28,96	150,13	7,50
	present TBT	31,65	37,59	7,03	28,96	150,38	7,03
	CBT [10]	28,78	37,50	-	28,78	150,00	-
	present CBT	28,78	37,59	-	28,78	150,38	-
	TSDBT	-	-	7,50	-	-	7,50
1	Li et al [9]	62,59	58,83	7,50	58,04	232,05	7,50
	present TBT	62,54	58,12	5,91	57,99	232,53	5,91
	CBT [10]	57,74	58,95	-	57,74	231,83	-
	present CBT	57,69	58,12	-	57,69	232,53	-
	TSDBT	-	-	7,50	-	-	7,50
2	Li et al [9]	80,60	68,81	6,38	74,41	270,98	6,38
	Present TBT	80,18	67,87	5,07	74,28	271,52	5,07
	CBT [10]	74,00	67,67	-	74,00	270,70	-
	present CBT	73,89	67,87	-	73,89	271,52	-
	TSDBT	-	-	6,38	-	-	6,38
5	Li et al [9]	97,80	81,03	5,12	88,15	318,11	5,12
	Present TBT	96,33	79,66	5,04	87,92	318,69	5,04
	CBT [10]	87,50	79,42	-	87,50	317,71	-
	Present CBT	87,36	79,66	-	87,36	318,69	-
	TSDBT	-	-	5,12	-	-	5,12

The calculated values based on the present theories (TBT, CBT) are obtained, it can be observed that the values obtained using the TBT and CBT) are in good agreement with those given by Li et al. [9] and Tai et al.[10] for all values of power law index and span-to-depth ratio.

It is worth noting that the results of Li et al. [9] are evaluated based on the analytical solutions (seen the Appendix B in the Ref Li et al. [9]).

It can be seen that the increasing of power law index will reduce the stiffness of the FG beams, and consequently, leads to an increase in the deflections and axial stress. This is due to the fact that higher values of power law index correspond to high portion of metal in comparison with the ceramic part, thus makes such FG beams more flexible.

For the case of transverse shear stress  $\tau_{xz}$ , the third order shear deformation theory (TSDBT) gives identical results

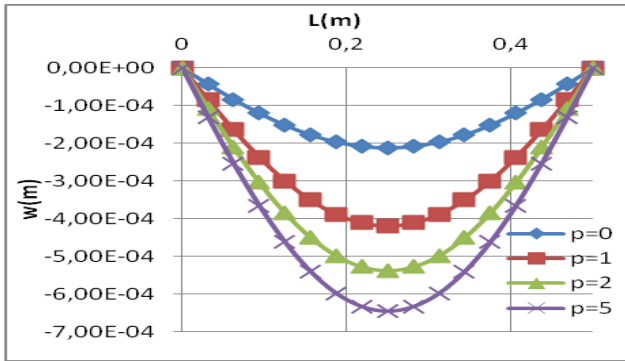
compared with Li et al. [9] unlike TBT. It can be explained by the different transverse shear strain shape functions used in each models.

Classical Beam Theory CBT:  $f(z)=0$

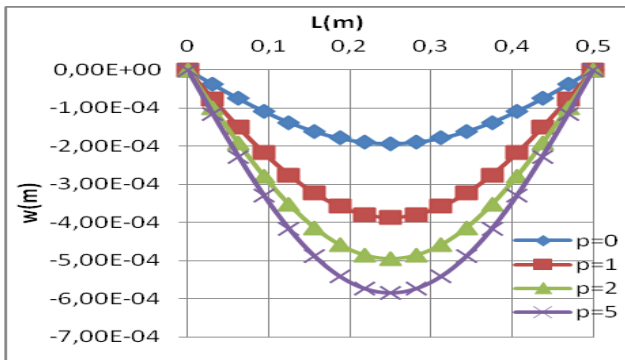
First order Shear Deformation Beam Theory TBT:  $f(z)=z$

Third order Shear Deformation Beam Theory TSDBT:

$$f(z) = z \left( 1 - \frac{4z^2}{3h^2} \right)$$

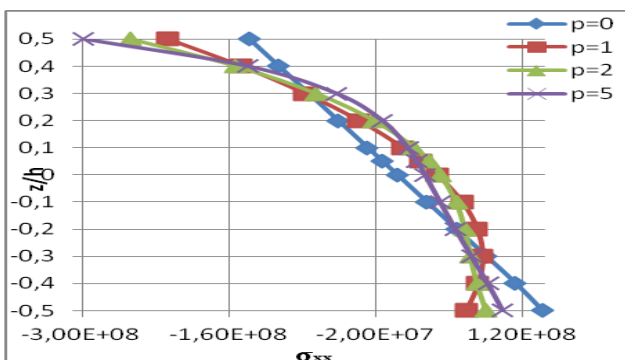


a) TBT

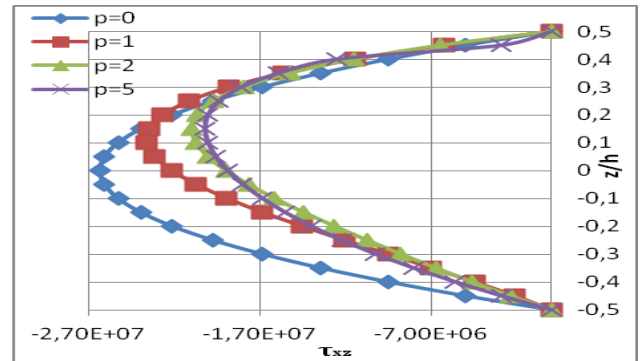


b) CBT

Figure 03: Transverse deflection along the beam length for  $L/h=5$  [a) TBT, b) CBT]

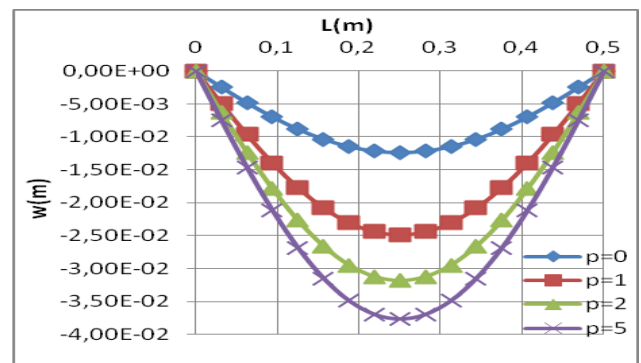


a)

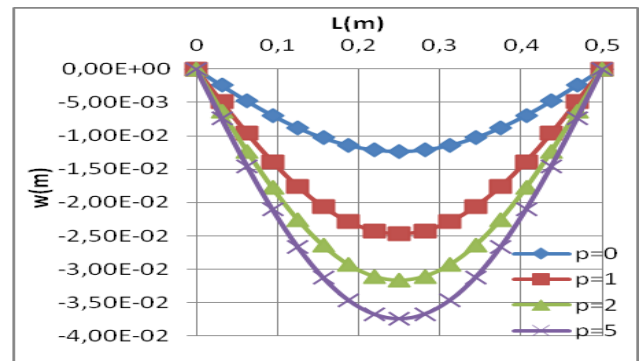


b)

Figure 04: Depthwise axial stresses and shear stresses distribution for  $L/h=5$

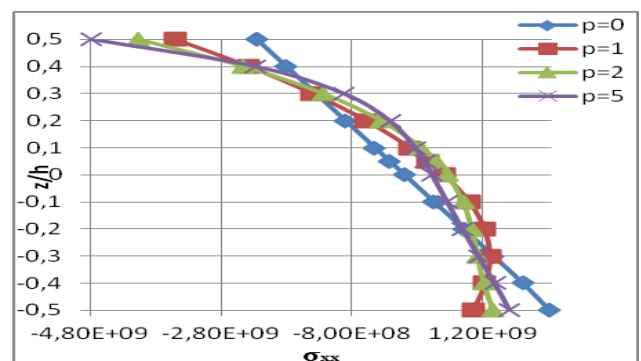


a) TBT



b) CBT

Figure 05: Transverse deflection along the beam length for  $L/h=20$  [a) TBT, b) CBT]



a)

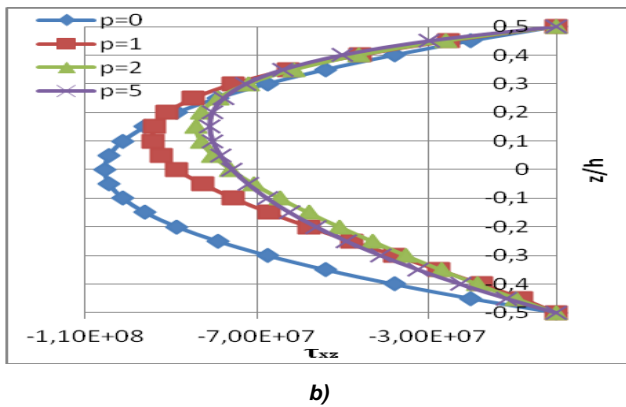


Figure 06: Depthwise axial stresses and shear stresses distribution for  $L/h=20$

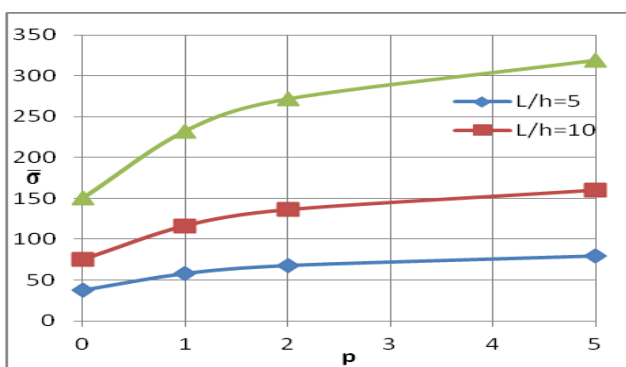


Figure 07: Variation of nondimensional axial normal stress with respect to the power law index  $p$  for FGM beams under uniform load

### 3.2 Comparison study

In this section, the deflection of the  $Al/Al_2O_3$  FGM beam using different beam theories will be investigated and compared. To facilitate a direct comparison, the obtained results are plotted in Fig. 3. And Fig.5 for  $L/h = 5$  and  $L/h = 20$ , respectively.

It can be noticed that deflections obtained from first order shear deformation theory are more important compared with given by classical beam theory; this is due simply to the presence of the transverse shear effect. Classical beam theory deals only simple bending, without considering the shear effect.

### 3.3 Effect of material parameter $p$ , on deflection, axial stress and shear stress

The deflection of the beam is shown in Fig. 3 and Fig.5 for various power law exponent,  $p$  and for different length-to-thickness ( $L/h=5$ ,  $L/h=20$  respectively). For  $Al/Al_2O_3$  FGM beam, transverse deflection increases as power law exponent  $p$  is increased.

As seen from (Fig .4.a) and (Fig.6.a) the axial stress distribution is linear for full ceramic and also the values of

tensile and compressive stresses are equal for isotropic beam (full ceramic). But for other values of  $p$  the axial stress distribution is not linear and also the values of compressive stresses are greater than tensile stresses, the value of axial stress is zero at the mid-plane but it is clearly visible that the values of axial stresses are not zero at the mid-plane of the FG beam for the other values of  $p$ ; it indicates that the neutral plane of the beam moves towards the upper side of the beam for FG beam. This is due to the variation of the modulus of elasticity through the thickness of the FG beam.

(Fig.4.b) and (Fig.6.b) depicts the variation of the shear stress across the thickness of beam. With increasing power law index ( $p$ ), the tip of shear stress decreases. By the way, it has not considerable effect on the distribution of shear stress.

In Fig.7, we used only TBT, it can be seen that the increasing of power law index leads to an increase in the axial stress.

## 4 CONCLUSION

In this paper, a finite element procedure for static analysis of functionally graded material (FGM) beam is presented. The material properties of the beam are assumed to vary continuously along the beam thickness by a power-law distribution. The assumed field displacements equations of the beam are represented by classical beam theory and first order shear deformation theories. A FORTRAN code is constructed to compute to predict the static responses .A simply supported beam subjected to uniform load for different length-to-thickness ratio has been chosen. The influences of span-to-depth and the volume fraction index on the mid plane deflections, and stresses distribution along the thickness of the beam are examined. The obtained results are compared with the existing solutions to verify the validity of the developed theories.

It was observed that the deflection increases as the power law index  $p$  increases. The axial stress distribution through the depth is linear when power law index value leads to a homogeneous beam (ceramic) ( $p=0$ ). For power law index other than homogeneous ( $p=1, 2$  and  $5$ ) composition the stress profile is not linear. The magnitude of maximum axial tensile stress and maximum axial compressive stress is dependent on the metal–ceramic combination. Distribution of transverse shear stress profile also depends on the metal–ceramic.

## REFERENCES

[1] Chakraborty, A., Gopalakrishnan, S., and Reddy, JN. (2003), A new beam finite element for the analysis of functionally graded materials, International Journal Mechanics Science, vol.45 (3), 519–539.

[2] Chakraborty, A. and Gopalakrishnan, S. (2003), A spectrally formulated finite element for wave propagation analysis in functionally graded beams, International Journal Solids Structures, vol.40 (10),

2421–2448

- [3] Kapuria, S., Bhattacharyya M., Kumar AN. (2008), Bending and free vibration response of layered functionally graded beams: A theoretical model and its experimental validation, *Composite Structures*, vol. 82(3): 390-402.
- [4] Kadoli, R., Akhtar K., Ganesan N. (2008), Static analysis of functionally graded beams using higher order shear deformation theory, *Applied Mathematical Modeling*, vol.32 (12), 2509-2525.
- [5] Shi, G., Lam K.Y., Tay T.E., (1998), On efficient finite element modeling of composite beams and plates using higher-order theories and an accurate composite beam element, *Computers and Structures*. Vol.41 159–165.
- [6] Kutiš, V., Murin J., Belak R., Paulech J., (2011), Beam element with spatial variation of material properties for multiphysics analysis of functionally graded materials, *Computers and Structures*. Vol.89 1192–1205.
- [7] Pindera, M-J., Dunn P. (1995), An Evaluation of Coupled Microstructural Approach for the Analysis of Functionally Graded Composites via the Finite Element Method, NASA CR 195455. Lewis Research Center, Cleveland, OH.
- [8] Nguyen, D.K., Gan, B.S. (2014), Large deflections of tapered functionally graded beams subjected to end forces”. *Applied Mathematical Modelling*, vol.38, 3054–3066
- [9] Li XF, Wang BL, Han JC. (2010), A higher-order theory for static and dynamic analyses of functionally graded beams, *Archive of Applied Mechanics*; 80(10):1197-1212.
- [10] Tai, H., Vo, T.(2012), Bending and free vibration of functionally graded beams using various higher-order shear deformation beam theories. *International Journal of Mechanical Sciences*, 62(1), 57-66.

## APPENDIX-A

### A. EULER BERNOULLI BEAM

The stiffness matrix of a general 2-D FGM beam element is

$$[K] = \begin{bmatrix} \frac{\hat{D}_a}{L} & 0 & \frac{-\hat{D}_{ab}}{L} & \frac{-\hat{D}_a}{L} & 0 & \frac{\hat{D}_{ab}}{L} \\ & \frac{12\hat{D}_b}{L^3} & \frac{6\hat{D}_b}{L^2} & 0 & \frac{-12\hat{D}_b}{L^3} & \frac{6\hat{D}_b}{L^2} \\ & & \frac{4\hat{D}_b}{L} & \frac{\hat{D}_{ab}}{L} & \frac{-6\hat{D}_b}{L^2} & \frac{2\hat{D}_b}{L} \\ & & & \frac{\hat{D}_a}{L} & 0 & \frac{-\hat{D}_{ab}}{L} \\ & & & & \frac{12\hat{D}_b}{L^3} & \frac{-6\hat{D}_b}{L^2} \\ & & & & & \frac{4\hat{D}_b}{L} \end{bmatrix} \quad (A1)$$

$$\begin{cases} \hat{D}_a = b \int_{-h/2}^{+h/2} E(z) dz \\ \hat{D}_b = b \int_{-h/2}^{+h/2} E(z) z^2 dz \\ \hat{D}_{ab} = b \int_{-h/2}^{+h/2} E(z) z dz \end{cases} \quad (A2)$$

Where: b is the width of the beam

$\hat{D}_a$  Is the axial stiffness  $\hat{D}_b$  is the bending stiffness,  $\hat{D}_{ab}$  is the coupling axial-bending stiffness.

$$\text{And } D = \frac{1}{L}$$

## APPENDIX-B

### B. TIMOSHENKO BEAM

The stiffness matrix of a general 2-D FGM beam element is

$$[K] = \begin{bmatrix} \frac{\hat{D}_a}{L} & 0 & \frac{-\hat{D}_{ab}}{L} & \frac{-\hat{D}_a}{L} & 0 & \frac{\hat{D}_{ab}}{L} \\ & \frac{12\hat{D}_b}{L^3(1+\phi_z)} & \frac{6\hat{D}_b}{L^2(1+\phi_z)} & 0 & \frac{-12\hat{D}_b}{L^3(1+\phi_z)} & \frac{6\hat{D}_b}{L^2(1+\phi_z)} \\ & & \frac{\hat{D}_{ab}(4+\phi_z)}{L(1+\phi_z)} & \frac{\hat{D}_{ab}}{L} & \frac{-6\hat{D}_b}{L^2(1+\phi_z)} & \frac{\hat{D}_b(2-\phi_z)}{L(1+\phi_z)} \\ & & & \frac{\hat{D}_a}{L} & 0 & \frac{-\hat{D}_{ab}}{L} \\ & & & & \frac{12\hat{D}_b}{L^3(1+\phi_z)} & \frac{-6\hat{D}_b}{L^2(1+\phi_z)} \\ & & & & & \frac{\hat{D}_b(4+\phi_z)}{L(1+\phi_z)} \end{bmatrix} \quad (B1)$$

From the equilibrium equation, we deduce  $\phi_z$

$$\phi_z = \frac{12\hat{D}_b}{L^2 K_z \hat{D}_s} \quad (B2)$$

With,

$$\hat{D}_s = K_z \hat{G}$$

$$\hat{D}_s = b \int_{-h/2}^{+h/2} G(z) dz$$

$$\hat{D}_a = b \int_{-h/2}^{+h/2} E(z) dz, \quad \hat{D}_{ab} = -b \int_{-h/2}^{+h/2} E(z) z dz, \quad \hat{D}_b = b \int_{-h/2}^{+h/2} E(z) z^2 dz$$

Where: b is the width of the beam.

$\phi_z$  is a coefficient which characterizes the transverse deformations. It depends on both the geometry and material characteristics of the section.

$\hat{D}_a$  Is the axial stiffness  $\hat{D}_b$  is the bending stiffness,  $\hat{D}_{ab}$  is the coupling axialbending stiffness,  $\hat{D}_s$  is the shear stiffness and  $K_z$  is the shear correction parameter for bending around the y axis.